

Available online at www.sciencedirect.com

ScienceDirect

journal homepage: www.elsevier.com/locate/ajps

Polymeric nanoparticles developed by vitamin E-modified aliphatic polycarbonate polymer to promote oral absorption of oleanolic acid



Wenjuan Zhang ^a, Chufan Liang ^b, Hao Liu ^c, Zhenbao Li ^a, Rui Chen ^a, Mei Zhou ^d, Dan Li ^a, Qing Ye ^a, Cong Luo ^{a,*}, Jin Sun ^{a,e,*}

^a School of Pharmacy, Shenyang Pharmaceutical University, No. 103, Wenhua Road, Shenyang 110016, China

^b HAISCO (Shenyang) Pharmaceutical Co. Ltd., Shenyang, China

^c School of Pharmacy, BioMolecular Sciences Department, The University of Mississippi, Oxford, MS 38677, USA

^d School of Continuing Education, Shenyang Pharmaceutical University, No. 103, Wenhua Road, Shenyang 110016, China

^e Municipal Key Laboratory of Biopharmaceutics, School of Pharmacy, Shenyang Pharmaceutical University, No. 103, Wenhua Road, Shenyang 110016, China

ARTICLE INFO

Article history:

Received 14 June 2017

Received in revised form 31 July 2017

Accepted 9 August 2017

Available online 12 October 2017

Keywords:

Oleanolic acid

Polymeric nanoparticles

mPEG-PCC-VE

Oral delivery

ABSTRACT

Oleanolic acid (OA) exhibited good pharmacological activities in the clinical treatment of hypoglycemia, immune regulation, acute jaundice and chronic toxic hepatitis. However, the oral delivery of OA is greatly limited by its inferior water solubility and poor intestinal mucosa permeability. Herein, we developed a novel polymeric nanoparticle (NP) delivery system based on vitamin E modified aliphatic polycarbonate (mPEG-PCC-VE) to facilitate oral absorption of OA. OA encapsulated mPEG-PCC-VE NPs (OA/mPEG-PCC-VE NPs) showed uniform particle size of about 170 nm with high drug loading capability (8.9%). Furthermore, the polymeric mPEG-PCC-VE NPs, with good colloidal stability and pH-sensitive drug release characteristics, significantly enhanced the *in vitro* dissolution of OA in the alkaline medium. The *in situ* single pass intestinal perfusion (SPIP) studies performed on rats demonstrated that the OA/mPEG-PCC-VE NPs showed significantly improved permeability in the whole intestinal tract when compared to OA solution, especially for duodenum and colon. As a result, the *in vivo* pharmacokinetics study indicated that the bioavailability of OA/mPEG-PCC-VE NPs showed 1.5-fold higher than commercially available OA tablets. These results suggest that mPEG-PCC-VE NPs are a promising platform to facilitate the oral delivery of OA.

© 2017 Shenyang Pharmaceutical University. Production and hosting by Elsevier B.V. This is an open access article under the CC BY-NC-ND license (<http://creativecommons.org/licenses/by-nc-nd/4.0/>).

* Corresponding authors. School of Pharmacy, Shenyang Pharmaceutical University, Shenyang 110016, China Tel.: +86 24 23986325.

E-mail addresses: luocong_0312@163.com (C. Luo); sunjin66@21cn.com (J. Sun).

Peer review under responsibility of Shenyang Pharmaceutical University.

<https://doi.org/10.1016/j.ajps.2017.08.003>

1818-0876/© 2017 Shenyang Pharmaceutical University. Production and hosting by Elsevier B.V. This is an open access article under the CC BY-NC-ND license (<http://creativecommons.org/licenses/by-nc-nd/4.0/>).

1. Introduction

Oral delivery is considered to be a preferred route for drug administration because of its convenience, painless administration, and high compliance with patients especially those in need of chronic therapies [1,2]. Drugs can maintain a sustained drug concentration in the circulation to increase the therapeutic efficiency [1]. However, multiple barriers hinder the oral administration of drugs due to their poor bioavailability, including physicochemical properties of drugs, physiological barriers in GI tract and biochemical barriers in GI tract [3]. At present, a wide range of oral drug delivery strategies to overcome the multiple barriers have been developed to enhance the stability of drugs, extend the GI tract residence time of drugs and carriers and promote the transport of drugs through the membrane of GI tract [2,3].

Oleanolic acid (OA) is a bioactive pentacyclic triterpenoid compound extracted from the leaves of *Olea europaea* L (also known as olea fruit) and clove, *swertia mileensis*, *prunella vulgaris* and *jujube* [4–6]. It is widely used in the therapy of hepatoprotective, anti-oxidation, two-way immune regulation, hypolipidemic, hypoglycemic, anti-tumor and acute jaundice and chronic toxic hepatitis in clinical due to high pharmacological activity and low side-effect [4,5,7–11]. OA belongs to the Class IV in Biopharmaceutics Classification System (BCS), with poor solubility and permeability. Therefore the inferior aqueous solubility and poor permeability across the intestinal tract [12], and accompanying low bioavailability [13] provide a daunting obstacle to OA wide appliance.

In order to facilitate oral delivery of OA, several attempts have been made to improve its bioavailability, such as nanosuspensions [14–16], β -cyclodextrin inclusion compounds, self-nanoemulsified formulations [17], phospholipid complexes [18–20], solid dispersions [21,22], and nanoparticles (NPs) [23,24]. Among them, polymeric NPs represent as a wide-applied drug delivery system by feat of better stability, versatile functionality and negligible adverse effects [25].

In the present study, a novel reported vitamin E modified aliphatic polycarbonate (mPEG-PCC-VE) polymer was employed to prepare NPs for oral delivery of OA. The prepared OA encapsulated mPEG-PCC-VE NPs (OA/mPEG-PCC-VE NPs) were characterized by a series of parameters including particle size, transmission electron microscope (TEM), differential scanning calorimetry (DSC), X-ray powder diffraction (XRPD), colloidal stability and dissolution profile. In addition, the *in situ* single pass intestinal perfusion (SPIP) and *in vivo* pharmacokinetics of the OA/mPEG-PCC-VE NPs were also evaluated. Our results clearly indicate a significant enhancement of permeability in the whole intestinal tract and an improved oral bioavailability of OA in the form of OA/mPEG-PCC-VE NPs as compared to commercial tablets after oral administration in rats.

2. Materials and methods

2.1. Materials

OA was purchased from Wuhan Dahua Pharmaceutical Co., Ltd. (Wuhan, Hubei). The chemical synthesis of mPEG-PCC-VE has

been reported in our previous study [26]. HPLC grade of tetrahydrofuran was purchased from Concord Technology (Tianjin) Co., Ltd. (Tianjin, China). H_3PO_4 (HPLC grade) was obtained from Tianjin Kemiou Chemical Reagent Co., Ltd. (Tianjin, China). Methanol of HPLC grade was purchased from Thermo Fisher Scientific (Shanghai, China).

2.2. Preparation of OA/mPEG-PCC-VE NPs

The OA/mPEG-PCC-VE NPs were prepared by the emulsion solvent evaporation method. Briefly, OA was dissolved in tetrahydrofuran, then 1 ml resultant solution was added in 10 mg mPEG-PCC-VE. After stirring at room temperature, the mixture was dropped into water slowly and stirred. Then the mixture was sonicated by a probe-type sonifier (JY92-2D, Scientz, China) for 10 min in ice bath, and organic solvents were removed in a rotary evaporator under vacuum. After centrifuging for 10 min at 13000 rpm, the upper layer was filtered through a 0.45 μ m filter membrane, then the OA/mPEG-PCC-VE NPs were obtained.

2.3. Characterization of OA/mPEG-PCC-VE NPs

2.3.1. Particle size and zeta potential

The particle size and size distribution of the prepared OA/mPEG-PCC-VE NPs were measured with dynamic light scattering (DLS) method by a Malvern Instruments Zetasizer (Nano ZS, Malvern Co., UK), and the measurements were repeated in triplicate.

2.3.2. Morphology

The morphology of OA/mPEG-PCC-VE NPs was observed by transmission electron microscope (TEM) (H-600, Hitachi, Japan). The particles were stained by 1.0% (w/v) phosphotungstic acid for 3 min on a copper grid stabilized with carbon support film.

2.3.3. DSC

DSC curves of OA, blank carrier material (mPEG-PCC-VE), physical mixture of OA and mPEG-PCC-VE were obtained using a DSC1 STAR[®] system (Mettler Toledo, Switzerland). The samples (3.0–5.0 mg) were weighted accurately, sealed into aluminum pans separately and heated from 20 to 340 °C at a heating rate of 10 °C/min. Plots of weight versus temperature were recorded. The DSC results were analyzed using the STAR^e software.

2.3.4. XRPD

XRPD analysis was performed on a D\Max-2400 X-Ray powder diffractometer (Rigaku, Japan) at ambient temperature. Monochromatic Cu-K α radiation ($\lambda = 1.5406 \text{ \AA}$) was used in the 2θ angle range from 3° to 50° with a step width of 0.05° at a voltage of 45 kV and current of 30 mA.

2.4. Colloidal stability of OA/mPEG-PCC-VE NPs

To investigate the colloidal stability of OA/mPEG-PCC-VE NPs in intestinal fluids, the prepared NPs were incubated at 37 °C with gentle shaking for 48 h. At regular intervals, the average particle size was determined by Malvern Instruments Zetasizer.

2.5. Determination of drug encapsulation efficiency and drug loading

2.5.1. RP-HPLC analysis

A Waters HPLC system including Pump e2695 Separations Module and Waters 2489 UV/Visible Detector (Waters Corp., Milford, MA, USA) was used to determine the concentrations of OA. A COSMOSIL 5 C18-AR-II column (150 mm × 4.6 mm, 5 μm) was used for the separation. Mobile phase composed of methanol and purified water containing 0.1% phosphoric acid (90:10, v/v) was used at a flow rate of 1.0 ml/min. The column temperature was maintained at room temperature. The wavelength of the UV detector was set at 210 nm. The calibration curve of OA concentrations (C, 4.09–204.5 μg/ml) versus integrated area (A, mAU) was plotted and the linear fit $A = 9238.8C + 4458.3$ was obtained with a correlation coefficient of 0.9998.

2.5.2. Encapsulation efficiency and drug loading

OA/mPEG-PCC-VE NPs were dissolved and diluted with methanol and dispersed by ultrasound, which disrupted the NP structure to release OA. The drug loading (DL) and encapsulation efficiency (EE) of OA in the prepared NPs were evaluated by determining the encapsulated OA using the RP-HPLC method. Each measurement was carried out in triplicate, and the EE and DL of NPs were calculated by following equations:

$$EE(\%) = \frac{S}{T} \times 100\%$$

$$DL(\%, w/w) = \frac{W_{OA}}{W_{Nano}} \times 100\%$$

where S is the amount of OA in the centrifugal supernatant, T is the total amount of OA added in the preparation, W_{OA} is the weight of OA in the freeze-dried OA/mPEG-PCC-VE NPs, W_{Nano} is the weight of the freeze-dried OA/mPEG-PCC-VE NPs.

2.6. In vitro drug release

The *in vitro* release performance of OA/mPEG-PCC-VE NPs was determined on a dissolution apparatus according to the paddle method described in the China pharmacopoeia (2015 edition). The dissolution medium was 900 ml deionized water containing 0.3% sodium dodecyl sulfate (SDS) [27]. The paddle speed was set to 100 rpm and the water bath temperature was maintained at 37 ± 0.5 °C. Samples (3 ml) of dissolution medium were withdrawn at 5, 10, 15, 20, 30, 45, 60, 90 and 120 min, and replaced with the same volume of fresh medium. The withdrawn samples were then filtered by 0.1 μm filter membrane and analyzed by HPLC at 210 nm. The dissolution data was modeled by DDSolver software [28].

2.7. In situ SPIP study of OA/mPEG-PCC-VE NPs

Healthy male Sprague–Dawley rats were obtained from the animal center of Shenyang Pharmaceutical University. The animal studies were approved by the Shenyang Pharmaceutical University Animal Care and Use Committee. Sprague–Dawley rats were fasted overnight with having access to water

before perfusion experiment. After intraperitoneal injection of 20% urethane (1.0 g/kg), rats were restrained on a warming pad to keep body temperature. Then a gentle incision along medioventral line was opened, and intestinal segments including duodenum, jejunum, ileum, and colon were recognized and pulled out carefully. Each intestinal segment was chosen about 10 cm, rinsed with freshly saline and balanced at a constant flow rate (Q) of 0.2 ml/min using peristaltic pump. The OA/mPEG-PCC-VE NPs were diluted to a final concentration equivalent to 20 μg/ml of OA. The intestinal perfusion lasted for 90 min, and all perfusion solution was collected. Finally the animal was sacrificed and the length (l) and radius (r) of the infused segments were measured precisely. The absorption rate constant (K_a) and apparent absorption coefficient (P_{app}) of OA was calculated by gravimetric method according to following equations:

$$K_a = \left(1 - \frac{C_{out}}{C_{in}} \cdot \frac{V_{out}}{V_{in}}\right) \cdot \frac{Q}{V}$$

$$P_{app} = \frac{-Q \cdot \ln\left(\frac{C_{out}}{C_{in}} \cdot \frac{V_{out}}{V_{in}}\right)}{2\pi r l}$$

where C_{out} is the OA concentration in the receptor tube, V_{out} is the OA perfusion solution volume in the receptor tube, C_{in} is the OA concentration in the donor solution, V_{in} is the OA perfusion solution volume in the donor solution, Q is the perfusion flow rate, r is the intestinal radius and l is the length of infusion segment.

2.8. In vivo pharmacokinetic study

To evaluate the oral bioavailability of OA/mPEG-PCC-VE NPs, *in vivo* pharmacokinetic study was carried out on Sprague–Dawley rats (200–250 g) according to the Guide for Care and Use of Laboratory Animals of Shenyang Pharmaceutical University. Sprague–Dawley rats were randomly divided into two groups, and the animals were fasten overnight with free access to water prior to the experiments. The suspensions of OA commercial tablets (20 mg/kg) and OA/mPEG-PCC-VE NPs (12 mg/kg) were administrated orally to rats, respectively. Blood samples (0.3 ml) were collected at 10 min, 20 min, 30 min, 45 min, 1 h, 1.5 h, 2 h, 4 h, 6 h, 8 h, 10 h, 12 h and 24 h from the retro-orbital plexus under mild anesthesia after intragastric administration. Plasma was obtained by centrifuging the blood samples at 13000 rpm for 10 min and stored at –20 °C. The concentrations of OA in rat plasma were determined by a validated UPLC–MS–MS method.

The main pharmacokinetic parameters were calculated using DAS 2.1 software, and the relative bioavailability (F_{rel}) was calculated according to following equation:

$$F_{rel}(\%) = \frac{AUC_{NPs} \cdot D_{CTS}}{AUC_{CTS} \cdot D_{NPs}} \times 100\%$$

where AUC_{NPs} is the area under curve of the prepared NPs, AUC_{CTS} is the area under curve of the commercial tablets, D_{NPs} is the dosage of the prepared NPs and D_{CTS} is the dosage of the commercial tablets.

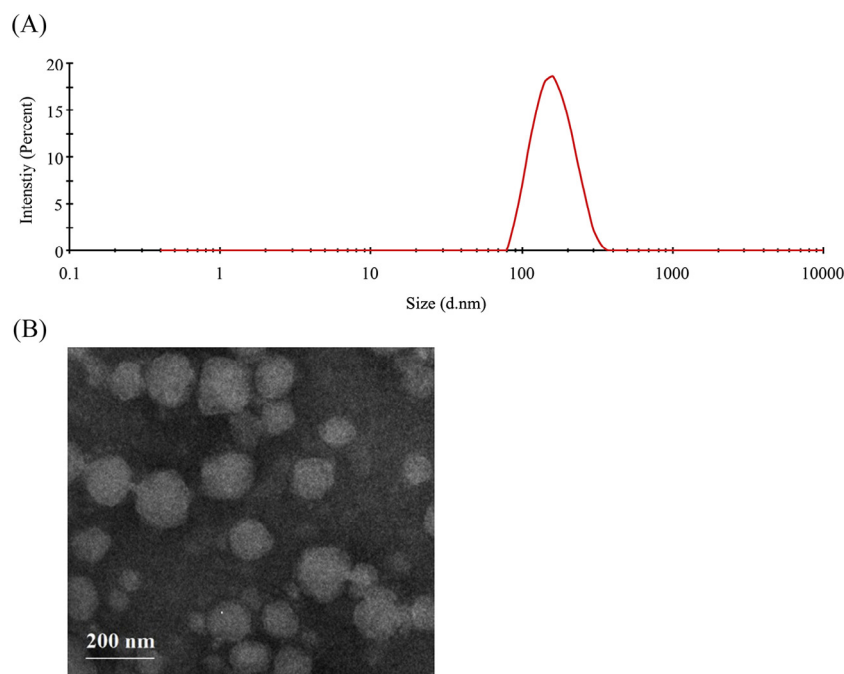


Fig. 1 – Particle size distribution (A) and TEM micrographs (B) of OA/mPEG-PCC-VE NPs.

3. Results and discussion

3.1. Preparation of OA/mPEG-PCC-VE NPs

Emulsion solvent evaporation method was used to prepare the OA/mPEG-PCC-VE NPs at a drug-to-carrier ratio of 1:1.5 (*w/w*). After the performance of the hydration temperature was set at 25 °C, ultrasonic power 200 W and ultrasonic time 10 min, we can obtain NPs of uniform size distribution, satisfactory EE (71%) and DL (8.9%).

The particle size and PDI value of OA/mPEG-PCC-VE NPs were evaluated by a dynamic light scattering system. As shown in Fig. 1A, the mean particle diameter of OA/mPEG-PCC-VE NPs was 165.06 ± 1.08 nm, and the PDI value was 0.131 ± 0.058 , indicating a narrow size distribution.

In addition, the stability of OA/mPEG-PCC-VE NPs in terms of size and PDI was shown in Fig. 2, which indicated that OA/mPEG-PCC-VE NPs were stable when stored at 37 °C for 42 h. However, PDI of OA/mPEG-PCC-VE NPs increased obviously when stored for 48 h due to some of the particles breaking and reaggregating.

3.2. Characterization of OA/mPEG-PCC-VE NPs

TEM was used to observe the morphology of OA/mPEG-PCC-VE NPs. As shown in Fig. 1B, the TEM images directly visualized the spherical structures of OA/mPEG-PCC-VE NPs.

The DSC curves of OA, mPEG-PCC-VE (Blank), OA and mPEG-PCC-VE complex (Physical mixture) and OA/mPEG-PCC-VE NPs were shown in Fig. 3. A sharp endothermic peak at 311.2 °C for the crude OA, indicative of its anhydrous and crystalline state.

However, the endothermic peak of OA disappeared in the DSC curve of OA/mPEG-PCC-VE NPs, indicating that OA existed in the NPs as amorphous state.

XRPD pattern was exploited to assess the crystal form of OA in OA/mPEG-PCC-VE NPs. The XRPD patterns of OA, Blank, Physical mixture and OA/mPEG-PCC-VE NPs were shown in Fig. 4. OA had intense diffraction peaks at 8.43, 12.99, 13.68, 15.36, 19.56 and 20.97°, suggesting that OA was present in crystalline form. However, there were no diffraction peaks of OA in OA/mPEG-PCC-VE NPs, suggesting almost complete drug amorphization.

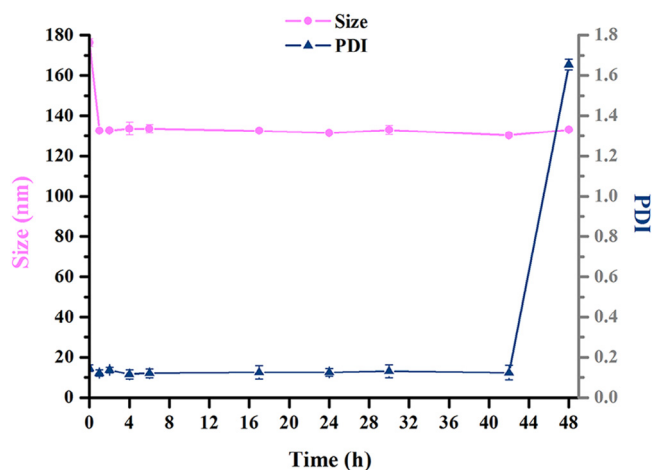


Fig. 2 – Stability of OA/mPEG-PCC-VE NPs in terms of size and PDI during 48 h storing at 37 °C.

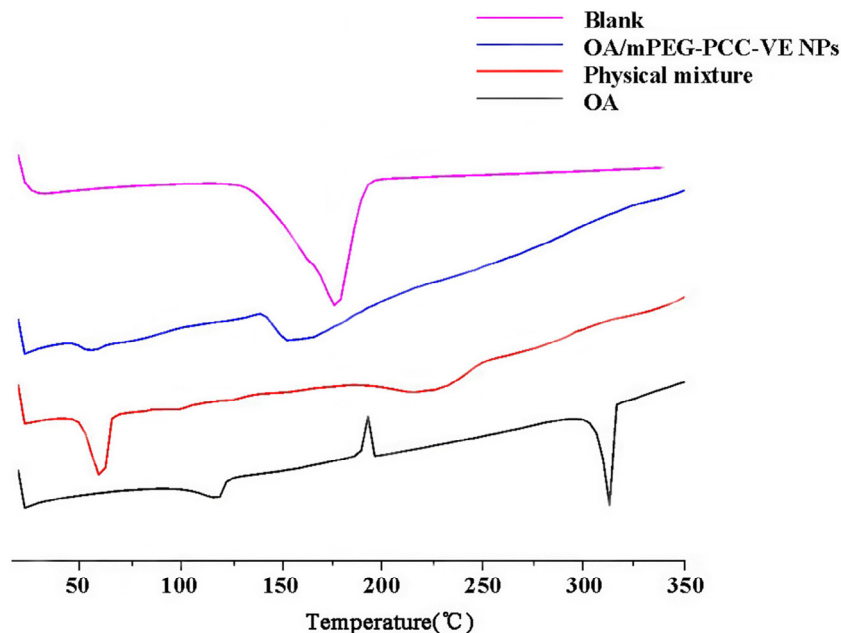


Fig. 3 – DSC thermograms of Blank (mPEG-PCC-VE), OA/mPEG-PCC-VE NPs, Physical mixture (OA+ mPEG-PCC-VE) and OA.

3.3. *In vitro* OA release profiles

Drugs have to dissolve in gastric and/or intestinal fluids before they can permeate the membranes of the GI tract to reach the systemic circulation. Thus, increasing the dissolution rate of poor aqueous solubility drugs is an important issue in pharmaceutical research [18]. The *in vitro* dissolution profiles of OA and OA/mPEG-PCC-VE NPs in 900 ml aqueous solution containing 0.3% (*w/v*) SDS were shown in Fig. 5. OA/mPEG-PCC-VE NPs showed a superior dissolution profile and the time for 78% drug dissolution was 30 min, while the dissolution for

physical mixture was only about 27% in the equal time. From the results, OA/mPEG-PCC-VE NPs dramatically improved the dissolution of OA. This could be explained by the special property of the carrier mPEG-PCC-VE which the ionized carboxyl groups favored the dissociation of the structure and the drug in cores would diffuse passively when it was in alkaline medium [23]. On the other hand, OA in the OA/mPEG-PCC-VE NPs was in an amorphous state, which enabled the drug to have higher internal energy and greater molecular motion, thus the dissolution of OA was improved. The modeling results established by DDSolve displayed in Table 1. Both the dissolution curves

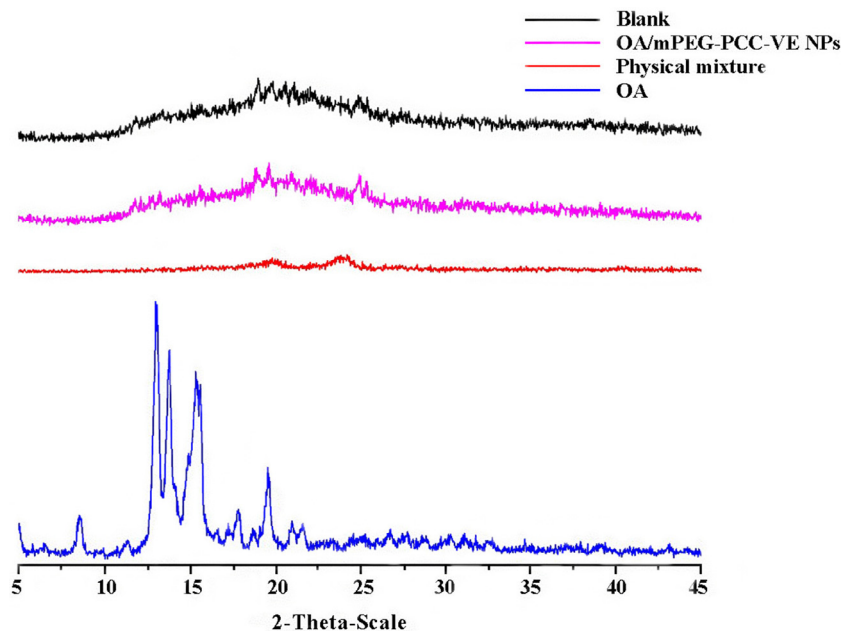


Fig. 4 – XRPD patterns of Blank (mPEG-PCC-VE), OA/mPEG-PCC-VE NPs, Physical mixture (OA+ mPEG-PCC-VE) and OA.

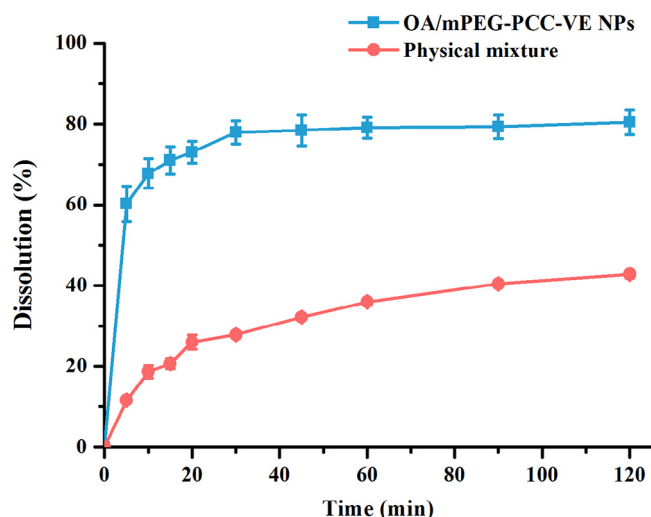


Fig. 5 – Dissolution profiles of (A) OA/mPEG-PCC-VE NPs, (B) Physical mixture (OA+ mPEG-PCC-VE).

of OA/mPEG-PCC-VE NPs and physical mixture conformed to the Weibull model ($r^2 = 0.9822, r^2 = 0.9880$).

3.4. In situ SPIP study of OA/mPEG-PCC-VE NPs

The *in situ* SPIP model in rats was used to evaluate the membrane permeability of OA/mPEG-PCC-VE NPs. As shown in Fig. 6, K_a and P_{app} of the OA/mPEG-PCC-VE NPs were significantly higher than those of OA solution in the whole intestinal segments, especially for colon and duodenum.

Since OA is a poorly water-soluble drug [18], a certain amount of sodium dodecyl sulfate was added in to improve the OA concentration of perfusion solution. According to our previous report [26], mPEG-PCC-VE as an orally nanosized carrier revealed enhanced the absorption in all segments of the intestine by confocal laser scanning microscope (CLSM), particularly colon exhibited the most absorption in a special mechanism, which was in an agreement with the K_a and P_{app} results in this study. What's more, OA is the substrate of CYP3A4 [29] which is widely distributed especially at duodenum, so it can also be absorbed specially by duodenum after prepared into NPs.

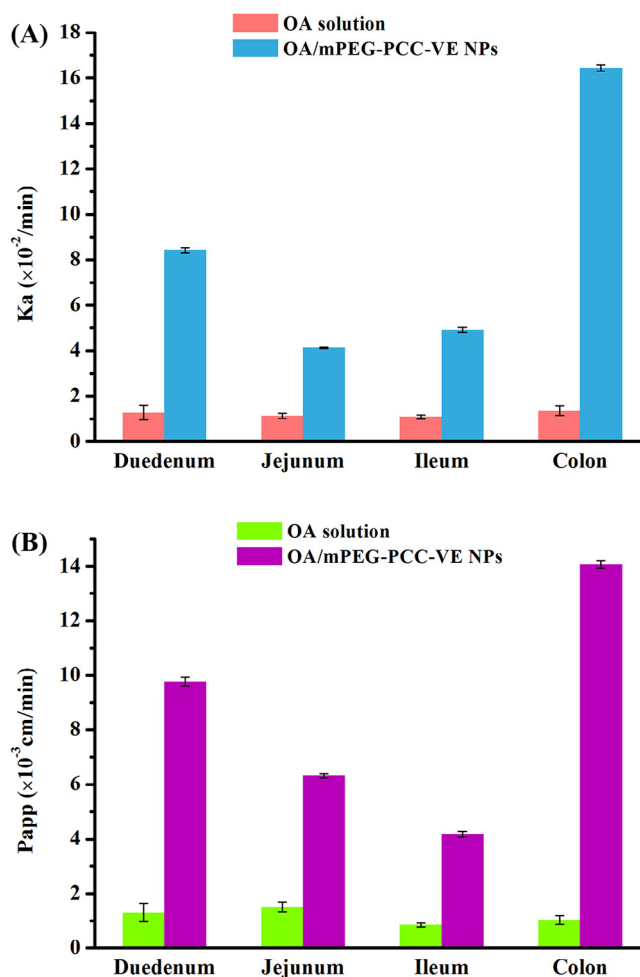


Fig. 6 – In situ SPIP, comparison of (A) K_a , (B) P_{app} of OA/mPEG-PCC-VE NPs and OA solution (data are mean \pm SD, $n = 3$).

3.5. In vivo pharmacokinetic study

The blood OA concentration versus time was shown in Fig. 7. The related pharmacokinetic parameters were displayed in Table 2. In comparison with the commercial tablets, the C_{max}

Table 1 – Release kinetics of physical mixture (OA+mPEG-PCC-VE) and OA/mPEG-PCC-VE NPs.

Models	Physical Mixture	OA/mPEG-PCC-VE NPs
Zero order	$y = 17.727 + 0.245x$ $r^2 = 0.8554$	$y = 68.410 + 0.131x$ $r^2 = 0.5702$
First order	$y = 43.311 \times (1 - e^{-0.028(x+8.552)})$ $r^2 = 0.9767$	$y = 79.673 \times (1 - e^{0.0081(x+13.018)})$ $r^2 = 0.9822$
Higuchi	$y = 7.722 + 3.451 \times x^{0.5}$ $r^2 = 0.9508$	$y = 62.239 + 1.980 \times x^{0.5}$ $r^2 = 0.7323$
Weibull	$y = 585.620 \times \left(1 - e^{-\frac{(x-2.696)^{0.414}}{57.038}}\right)$ $r^2 = 0.9880$	$y = 79.994 \times \left(1 - e^{-\frac{(x+8.119)^{0.765}}{10.429}}\right)$ $r^2 = 0.9840$
Logistic	$y = \frac{41.718}{1 + e^{-0.049 \times (x-16.232)}}$ $r^2 = 0.9580$	$y = \frac{79.560}{1 + e^{-0.096 \times (x+7.606)}}$ $r^2 = 0.9807$

Table 2 – Pharmacokinetic parameters after oral administration of OA commercial tablets (20 mg/kg) and OA/mPEG-PCC-VE NPs formulations at a dose equivalent to 12 mg/kg OA, respectively (mean \pm SD, n = 5).

Preparations	Dosage (mg/kg)	$t_{1/2}$ (h)	C_{max} (ng/ml)	T_{max} (h)	AUC_{0-24h} (ng/ml*h)	F_{rel} (%)
Commercial tablets	20	20.9 \pm 15.3	40.15 \pm 23.33	0.667 \pm 0.56	321.98 \pm 128.36	100
OA/mPEG-PCC-VE NPs	12	24.67 \pm 17.48	28.07 \pm 13.89	0.729 \pm 0.55	295.59 \pm 112.7	153.01

of the group orally administrated the OA/mPEG-PCC-VE NPs was slightly improved. The F_{rel} of OA/mPEG-PCC-VE NPs was 153%, demonstrating that mPEG-PCC-VE NPs developed in this study significantly enhanced intestinal absorption and oral bioavailability of OA.

Compared with sucrose ester-stabilized nanosuspensions of OA (SEOA) [15], the pharmacokinetic parameters of the prepared OA/mPEG-PCC-VE NPs are improved, especially the $t_{1/2}$. The $t_{1/2}$ of the sucrose ester-stabilized OA nanosuspensions is about 78 min while the $t_{1/2}$ of the OA/mPEG-PCC-VE NPs is 24.67 h, which is a dramatic improvement. Moreover, the t_{max} and F_{rel} of OA/mPEG-PCC-VE NPs are also improved compared with those of OA-phospholipid complex-hydroxyapatite (OPCH) [18]. The t_{max} and F_{rel} of OPCH are 0.46 h and 139.4%, while the t_{max} and F_{rel} of OA/mPEG-PCC-VE NPs are 0.729 h and 153.01%, respectively. We may attribute the enhanced pharmacokinetic parameters to the special property of the mPEG-PCC-VE. It could form the nanosized particles, which may prolong the residence time in the intestinal tract by physical absorption.

4. Conclusions

The OA/mPEG-PCC-VE NPs developed by mPEG-PCC-VE polymer as an effective drug delivery system were successfully prepared by solvent evaporation method. As compared to the physical mixture, the mPEG-PCC-VE NPs could significantly improve the dissolution of OA. The OA/mPEG-PCC-VE NPs can

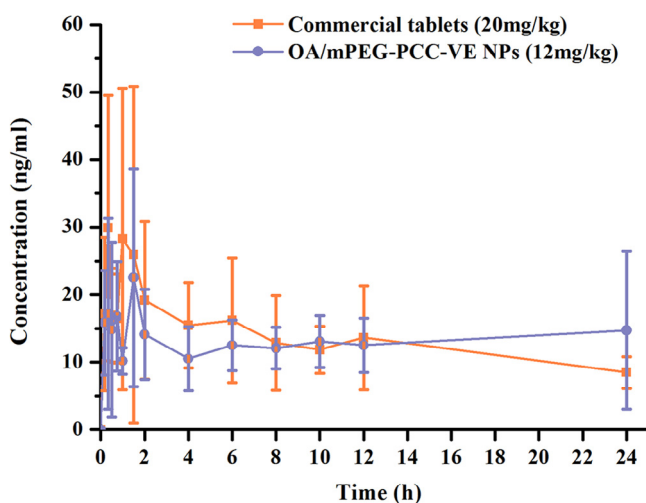


Fig. 7 – Mean plasma concentration-time curves of OA in rats after oral administration of commercial tablets and OA/mPEG-PCC-VE NPs (data are mean \pm SD, n = 5).

remarkably enhance the absorption of OA in intestinal tract, especially for duodenum and colon. After oral administration, the OA/mPEG-PCC-VE NPs showed higher C_{max} and AUC_{0-24h} in rat plasma. And the OA/mPEG-PCC-VE NPs exhibited a 1.53-fold increase in bioavailability when compared to the commercial available tablets. These results demonstrated that mPEG-PCC-VE NPs were a promising platform to facilitate the oral delivery of poorly water-soluble drugs.

Conflicts of interest

The authors declare that there are no conflicts of interest.

Acknowledgements

We are grateful to financial support from the National Natural Science Foundation of China, No. 81373336, 81473164.

REFERENCES

- [1] Feng S, Zhao L, Tang J. Nanomedicine for oral chemotherapy. *Nanomedicine (Lond)* 2011;6:407–410.
- [2] Mei L, Zhang Z, Zhao L, et al. Pharmaceutical nanotechnology for oral delivery of anticancer drugs. *Adv Drug Deliv Rev* 2013;65:880–890.
- [3] Luo C, Sun J, Du Y, et al. Emerging integrated nanohybrid drug delivery systems to facilitate the intravenous-to-oral switch in cancer chemotherapy. *J Control Release* 2014;176:94–103.
- [4] Liu J. Oleanolic acid and ursolic acid: research perspectives. *J Ethnopharmacol* 2005;100:92–94.
- [5] Pollier J, Goossens A. Oleanolic acid. *Phytochemistry* 2012;77:10–15.
- [6] Somova LI, Shode FO, Ramnandan P, et al. Antihypertensive, antiatherosclerotic and antioxidant activity of triterpenoids isolated from *Olea europaea*, subspecies *africana* leaves. *J Ethnopharmacol* 2003;84:299–305.
- [7] Liu J. Pharmacology of oleanolic acid and ursolic acid. *J Ethnopharmacol* 1995;49:57–68.
- [8] Junei K, Masafumi O, Manabu U, et al. Hepatoprotective and hepatotoxic actions of oleanolic acid-type triterpenoidal glucuronides on rat primary hepatocyte cultures. *Chem Pharm Bull* 1999;47:290–292.
- [9] Aruna K, Shalini S. Effect of oleanolic acid on complement in adjuvant- and Carrageenan-induced inflammation in rats. *J Pharm Pharmacol* 1995;47:585–587.
- [10] Ortiz AR, Garcia JS, Castillo EP, et al. Alpha-Glucosidase inhibitory activity of the methanolic extract from *Tournefortia hartwegiana*: an anti-hyperglycemic agent. *J Ethnopharmacol* 2007;109:48–53.

- [11] Hsu H, Yang J, Lin C. Effects of oleanolic acid and ursolic acid on inhibiting tumor growth and enhancing the recovery of hematopoietic system postirradiation in mice. *Cancer Lett* 1997;111:7–13.
- [12] Tong HHY, Wu HB, Zheng Y, et al. Physical characterization of oleanolic acid nonsolvate and solvates prepared by solvent recrystallization. *Int J Pharm* 2008;355:195–202.
- [13] Jeong DW, Kim YH, Kim HH, et al. Dose-linear pharmacokinetics of oleanolic acid after intravenous and oral administration in rats. *Biopharm Drug Dispos* 2007;28:51–57.
- [14] Li W, Ng KY, Heng PWS. Development and evaluation of optimized sucrose ester stabilized oleanolic acid nanosuspensions prepared by wet ball milling with design of experiments. *Biol Pharm Bull* 2014;37:926–937.
- [15] Li W, Das S, Ng KY, et al. Formulation, biological and pharmacokinetic studies of sucrose ester-stabilized nanosuspensions of oleanolic acid. *Pharm Res* 2011;28:2020–2033.
- [16] Chen Y, Liu J, Yang X, et al. Oleanolic acid nanosuspensions: preparation, in-vitro characterization and enhanced hepatoprotective effect. *J Pharm Pharmacol* 2005;57:259–264.
- [17] Xi J, Chang Q, Chan CK, et al. Formulation development and bioavailability evaluation of a self-nanoemulsified drug delivery system of oleanolic acid. *AAPS PharmSciTech* 2009;10:172–182.
- [18] Jiang Q, Yang X, Du P, et al. Dual strategies to improve oral bioavailability of oleanolic acid: enhancing water-solubility, permeability and inhibiting cytochrome P450 isozymes. *Eur J Pharm Biopharm* 2016;99:65–72.
- [19] Cao F, Gao Y, Yin Z, et al. Enhanced oral bioavailability of oleanolic acid in rats with phospholipid complex. *Lett Drug Des Discov* 2012;9:505–512.
- [20] Yang X, Jiang Q, Du P, et al. Preparation and characterization of solidified oleanolic acid–phospholipid complex aiming to improve the dissolution of oleanolic acid. *Asian J Pharm Sci* 2016;11:241–247.
- [21] Liu L, Wang X. Improved dissolution of oleanolic acid with ternary solid dispersions. *AAPS PharmSciTech* 2007;8: E113.
- [22] Tong HHY, Du Z, Wang GN, et al. Spray freeze drying with polyvinylpyrrolidone and sodium caprate for improved dissolution and oral bioavailability of oleanolic acid, a BCS Class IV compound. *Int J Pharm* 2011;404:148–158.
- [23] Alvarado HL, Abrego G, Garduno-Ramirez ML, et al. Design and optimization of oleanolic/ursolic acid-loaded nanoplatforms for ocular anti-inflammatory applications. *Nanomedicine (Lond)* 2015;11:521–530.
- [24] Man DK, Casettari L, Cespi M, et al. Oleanolic acid loaded PEGylated PLA and PLGA nanoparticles with enhanced cytotoxic activity against cancer cells. *Mol Pharm* 2015;12:2112–2125.
- [25] Meng F, Zhong Y, Heng R, et al. pH-sensitive polymeric nanoparticles for tumor-targeting doxorubicin delivery: concept and recent advances. *Nanomedicine (Lond)* 2014;9:487–499.
- [26] Wang M, Sun J, Zhai Y, et al. Enteric polymer based on pH-responsive aliphatic polycarbonate functionalized with vitamin E to facilitate oral delivery of tacrolimus. *Biomacromolecules* 2015;16:1179–1190.
- [27] Li Y, Liu H, Guo B, et al. Enhancement of dissolution rate and oral bioavailability in beagle dogs of oleanolic acid by adsorbing onto porous silica using supercritical carbon dioxide. *J Drug Deliv Sci Technol* 2014;24:380–385.
- [28] Zhang Y, Huo M, Zhou J, et al. DDSolver: an add-in program for modeling and comparison of drug dissolution profiles. *AAPS J* 2010;12:263–271.
- [29] Kim KA, Lee JS, Park HJ, et al. Inhibition of cytochrome P450 activities by oleanolic acid and ursolic acid in human liver microsomes. *Life Sci* 2004;74:2769–2779.